A LETTERS JOURNAL EXPLORING THE FRONTIERS OF PHYSICS

OFFPRINT

Pre-avalanche structural rearrangements in the bulk of granular medium: Experimental evidence

V. Yu. Zaitsev, P. Richard, R. Delannay, V. Tournat and V. E. Gusev

EPL, **83** (2008) 64003

TAKE A LOOK AT THE NEW EPL

Europhysics Letters (EPL) has a new online home at
www.epljournal.org

Take a look for the latest journal news and information on:

- reading the latest articles, free!
- receiving free e-mail alerts
- submitting your work to EPL

www.epljournal.org

A Letters Journal Exploring the Frontiers of Physics

September 2008

EPL, **83** (2008) 64003
doi: 10.1209/0295-5075/83/64003

www.epljournal.org

Pre-avalanche structural rearrangements in the bulk of granular medium: Experimental evidence

V. Yu. Zaitsev[1(a)], P. Richard[2], R. Delannay[2], V. Tournat[3] and V. E. Gusev[3]

[1] *Institute Applied Physics, Russian Academy of Sciences - Uljanova St. 46, 603950, Nizhny Novgorod, Russia*
[2] *Institut de Physique de Rennes - UMR CNRS 6251, Université Rennes-1 - 263 av. Général Leclerc, 35042, Rennes Cedex, France, EU*
[3] *LAUM, LPEC, CNRS, Université du Maine - av. Olivier Messiaen, 72085, Le Mans Cedex 9, France, EU*

received 28 April 2008; accepted in final form 31 July 2008
published online 10 September 2008

PACS 45.70.Ht – Avalanches
PACS 43.25.+y – Nonlinear acoustics
PACS 83.80.Fg – Granular solids

Abstract – Granular avalanches are typical threshold-type phenomena implying the loss of stability of granular packings when their slope exceeds a critical angle. Detection of avalanche precursors is important for both basic studies and numerous applications. In this respect, only surface observations are presently available, whereas other known techniques are not suitable to detect internal pre-avalanche rearrangements expected from physical considerations and numerical simulations. Here, we report the first experimental evidence of avalanche precursors and the long-lasting post-avalanche rearrangements in the bulk of 3D granular packings. We use an original nonlinear-acoustic probing methodology which is selectively sensitive to the state of weakest intergrain contacts. This methodology allowed us to clearly detect transient pre-avalanche rearrangements of the weak-contact network. Those rearrangements get stronger and exhibit quasi-periodicity closer to the avalanche triggering, whereas the statistics of the sounding signal amplitude shows clear transition from Gaussian to power law behavior.

Introduction. – Among the rich variety of intriguing effects observed in granular media [1,2], avalanche-type processes [3,4] are attracting much attention due to their interesting physics and importance in geophysics, numerous industrial and security-related applications. One can mention, for example, the huge landslide that destroyed a large part of the famous Geyser Valley at Kamchatka Peninsula in June 2007. Avalanches are typical threshold-type phenomena implying the loss of stability of a granular pile when its slope exceeds a critical angle, usually between 27° and 30°. The precise angle depends on fine features of the grain packing, which cannot be exactly reproduced in repetitive measurements. An important question is whether reliable precursors of the approaching critical state can be found. In such studies, various experimental techniques have been used, most of them based on mechanical measurements of the critical angles [1,3,4], which can be combined with tracking of grain rearrangements in 2D packings confined by transparent walls [1], in inclined granular monolayers [5,6] or on the pile surfaces [4,7,8]. The main finding is that with increasing tilt angle, the number of on-surface grain rearrangements gradually increases. Initially, for the pile slope $10^\circ - 20^\circ$, these events are weak and random. For the last $6^\circ - 8^\circ$ before the critical angle, much larger quasi-periodic (separated by intervals of $1^\circ - 2^\circ$) on-surface collective rearrangements-precursors were observed [8], which poses the question whether similar structural changes occur in the bulk of the material. In this context, numerical simulations [9,10] using contact-dynamics method [11] are known for 2D packings of cohesionless frictional discs. Results [9,10] indicated that for certain portions of the intergrain contacts, with gradually increasing tilt angle the tangential contact forces become larger than the dry-friction forces, *i.e.*, the dry friction is "mobilized". For such contacts, rapid rearrangements are numerically predicted [9,10]. These rearrangements or "precursors" increase in strength as the critical angle is approached.

Experimental verification of existence of such rapid micro-rearrangements in the material bulk is a challenging

(a) E-mail: vyuzai@hydro.appl.sci-nnov.ru

problem even for 2D grain packings, where the grains are visually accessible, and looks even more complicated for the grains in the material bulk. Known and otherwise very useful methods (*e.g.*, analysis of grain imprints on carbon paper [12] for studying contact forces, direct application of micro-balance [13] or stress visualization due to photo-elasticity [14,15], or probing grain piles by X-rays [16]) do not provide the necessary sensitivity to weak transient rearrangements, and do not allow measurements inside 3D media in real time with sufficient time resolution. Conventionally, acoustic probing of the medium bulk is based on the linear sound propagation controlled by the linear elastic moduli [17–21]. The latter are determined first of all by the network of average-loaded contacts, which persists and supports the medium up to the very threshold of the avalanche. Thus the acoustic probing of material's linear elastic moduli is insensitive to weakly loaded contacts, for which the pre-avalanche loss of stability can be expected first of all. The results presented below demonstrate exciting prospects opened in this field and related problems by the emerging nonlinear-acoustic technique.

In the present letter, we report the first experimental evidence of pre-avalanche rearrangements in the bulk of 3D granular packing. The applied unconventional technique exploits the intrinsic selective sensitivity of the nonlinearity-induced components of the probing acoustic signal to weakest contacts [22–26], making it an ideal tool to investigate these phenomena. In addition, this technique allowed us to reveal that such weak-contact rearrangements continue after the avalanche, suggesting that the time needed to obtain a truly equilibrium state even in small granular piles is of the order of tens of minutes.

Experimental methodology and conditions. – Nonlinear acoustic methods are an attractive tool for studying granular materials because the signal components arising from material nonlinearities are dominated by the contribution of the weakest contacts [22,23]. This fact contradicts the conventional "linear" intuition, which predicts that the stronger contacts give the maximal contribution to the acoustic signal. Existence of weak contacts is indicated by direct contact-force measurements [27] and numerical simulations [9,10,27]. Besides, for the compressional-wave velocity C as a function of the static stress σ_0, instead of $C \propto \sigma_0^{1/6}$ predicted by the Hertz law, normally a faster law $C \propto \sigma_0^{(1/4)-(1/5)}$ is observed. This discrepancy is attributed to gradual "activation" of initially unloaded contacts. Schematically, such average- and weakly-loaded contacts are shown as two neighbouring grain chains in fig. 1. Their initial static strains are ε_0 and $\mu\varepsilon_0$ (where we introduced the dimensionless parameter $\mu \ll 1$ which can be arbitrarily small due to small difference either in grain sizes or grain numbers). In contrast, the dynamic strains $\tilde{\varepsilon} \approx \tilde{h}/h_0$ are practically the same for both the groups of contacts.

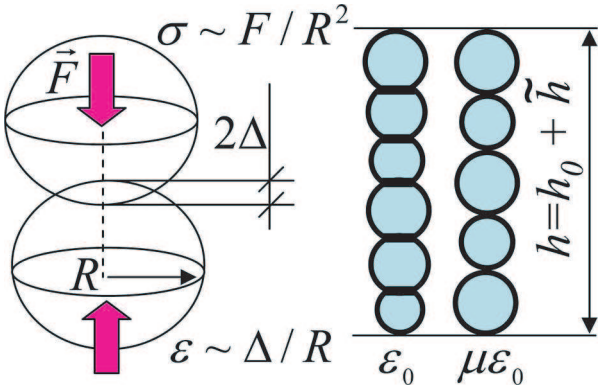

Fig. 1: Left: sketch of a single Hertzian contact showing the relation of its characteristics to the macroscopic stress and strain. Right: elucidation of the fact that for contact chains with strongly different static prestrains ε_0 and $\mu\varepsilon_0$, the dynamic (acoustic) strain $\tilde{\varepsilon} \approx \tilde{h}/h_0$ is practically the same. The introduced notations are clear from the figure.

The acoustic consequences of this can be elucidated using a simple model [25], which relates the static σ_0 and acoustic $\tilde{\sigma}$ stresses with the respective strain components ε_0 and $\tilde{\varepsilon} \ll \varepsilon_0$ for an ensemble of grains interacting via differently loaded Hertzian contacts:

$$\sigma_0 + \tilde{\sigma} = A(\varepsilon_0 + \tilde{\varepsilon})^{\frac{3}{2}} H(\varepsilon_0 + \tilde{\varepsilon}) + B(\mu\varepsilon_0 + \tilde{\varepsilon})^{\frac{3}{2}} H(\mu\varepsilon_0 + \tilde{\varepsilon}). \tag{1}$$

Here, like in [24], along with average-loaded contacts with static prestrain ε_0 we retain another fraction of weakly loaded contacts with prestrain $\mu\varepsilon_0$. Parameters A and B are proportional to the amounts of contacts in these fractions and the Heaviside functions $H(..)$ indicate that the contacts do not bear tensile loading. For moderate acoustic amplitudes $\tilde{\varepsilon} \ll \varepsilon_0$ but $\tilde{\varepsilon} > \mu\varepsilon_0$, the weak contacts may even clap, while the average-loaded packing skeleton still remains jammed. For an applied acoustic strain $\tilde{\varepsilon} = a\cos(\omega t)$, one can readily estimate from eq. (1) the amplitudes of the fundamental acoustic-stress harmonic $\tilde{\sigma}_\omega$ as well as the second harmonic $\tilde{\sigma}_{2\omega}$ (or the demodulated harmonic $\tilde{\sigma}_\Omega$ if the acoustic-strain amplitude a is slowly modulated, for example, $a(t) = a[1 + \cos(\Omega t)]$). For sufficiently small amplitudes $\tilde{\varepsilon} \ll \mu\varepsilon_0$ (when even weak contacts do not clap), eq. (1) can be expanded into power series, which allows us to analytically estimate $\tilde{\sigma}_\omega$ as well as $\tilde{\sigma}_{2\omega}$ and $\tilde{\sigma}_\Omega$:

$$\tilde{\sigma}_\omega \propto A\sqrt{\varepsilon_0}\left[1 + \frac{B\sqrt{\mu}}{A}\right]\tilde{\varepsilon}, \quad \tilde{\sigma}_{2\omega,\Omega} \propto \frac{A}{\sqrt{\varepsilon_0}}\left[1 + \frac{B}{A\sqrt{\mu}}\right]\tilde{\varepsilon}^2. \tag{2}$$

Expressions (2) clearly demonstrate the opposite roles of differently loaded contacts in the generation of $\tilde{\sigma}_\omega$ and $\tilde{\sigma}_{2\omega,\Omega}$ signal components. Weak contacts with $\mu \ll 1$ give negligible contribution to the fundamental harmonic $\tilde{\sigma}_\omega$ (since $\sqrt{\mu} \ll 1$). In contrast, their contribution to the nonlinearity-induced components $\tilde{\sigma}_{2\omega,\Omega}$ is strongly dominant ($1/\sqrt{\mu} \gg 1$). Thus the level of the

nonlinearity-induced signal component can give almost pure information on the variability of the weak-contact parameters. More rigorously, the nonlinear-signal level should be found by summing up contributions of nonlinear sources over the volume insonified by the primary radiated acoustic beam [25]. However, here we limit ourselves to the discussion of the local nonlinear sources, for which eqs. (2) valid for $\tilde{\varepsilon} < \mu\varepsilon_0$ clearly show the difference in the relative contributions of the average-loaded and the weakly-loaded contacts to the nonlinearity-induced signal components. The level of $\tilde{\sigma}_{2\omega,\Omega}$ for larger amplitudes $\mu\varepsilon_0 < \tilde{\varepsilon} \ll \varepsilon_0$ (including the clapping regime of the weak contacts, which is interesting in practice to increase the nonlinear signal level) can be readily estimated using the initial eq. (1). The generation of $\tilde{\sigma}_{2\omega}$ and $\tilde{\sigma}_\Omega$ components was recently successfully used to evaluate the weak-contact portion in packings of spherical glass beads [24,25]. According to these data, for moderately compressed granular packings (*e.g.* for pressure $\leqslant 10^4$ Pa), a rather significant fraction of the contact forces falls into the range below a few percent of the average value (*i.e.*, for such contacts, the unloading parameter μ is $\sim 10^{-2}$). This force range is practically inaccessible to other techniques, especially for observation of rapid transitional phenomena.

Concerning the avalanche preparation, it is important that the weak-contact fraction is the most sensitive to any perturbations of the grain state. In particular, when oblique contacts forces in the slowly tilted packing reaches the dry-friction threshold, such activated contacts jump into a neighboring position breaking the intergrain contact for a short time. Sufficiently far from the critical angle, such jumps-rearrangements are uncorrelated and concern only a small contact portion. Then the number of activated contacts increases, so that the stability lost for one contact can affect the neighboring nearly-activated contacts, thus producing collective rearrangement. Then such contacts again accumulate the tangential load and exhibit another collective rearrangement, which resembles periodic frictional stick-slip motion at solid-solid interfaces. This intuitively clear scenario well agrees with the 2D simulation [9,10].

Using eq. (1) we may readily compare the variability of $\tilde{\sigma}_\omega$ and $\tilde{\sigma}_\Omega$ or $\tilde{\sigma}_{2\omega}$ due to such processes. Assuming that portion B of the weak contacts equals 0.4 of the total number of all contacts (which is consistent with data [24,25]), we consider a gradually increasing number B_a of the mobilized (*i.e.*, experiencing rearrangements jumps) weak contacts and a correspondingly decreasing number B_s of stable weak contacts: $B_a = B_a^{(0)} + \Delta B\theta$ and $B_s = B_s^{(0)} - \Delta B\theta$, where θ is the current tilt angle and ΔB is assumed positive. In the example below, we assume for the illustration that the portion of mobilized weak contacts gradually increases from 10 to 30 percents of their total number $B = B_s + B_a$, *i.e.* initially $B_a^{(0)} = 0.1$ and parameter B_a ranges from 0.1 to 0.3. Bearing in mind the periodic scenario described above, we approximate the variation of parameter μ by the dependence

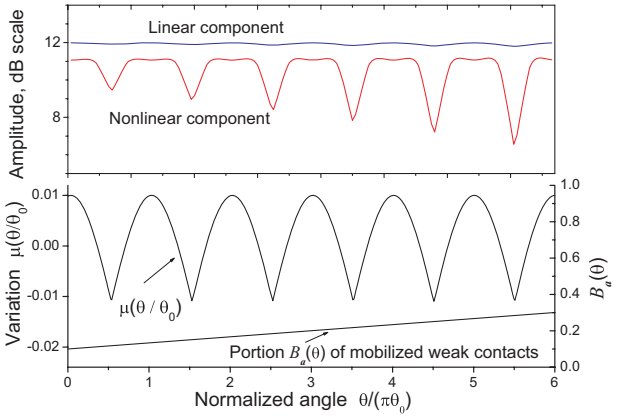

Fig. 2: Predicted by eq. (1) simultaneous variations in the fundamental ($\tilde{\sigma}_\omega$) and nonlinear ($\tilde{\sigma}_\Omega$ or $\tilde{\sigma}_{2\omega}$) signal components (upper plot) induced by perturbations of the weak-contact fraction with unloading parameter $\mu = 0.01$. The lower plot shows $\mu(\theta)$ and gradually increasing amount $B_a(\theta)$ of activated weak contacts assuming amount $B = B_s + B_a$ of weak contacts being 40% of the total contact number in the packing, which agrees with data [24,25] obtained for similar granular materials.

$\mu(\theta) = \mu_0 - \Delta\mu[1 - |\cos(\theta/\theta_0)|]$, where parameter θ_0 characterizes the period of the collective contact rearrangements. For $\Delta\mu \geqslant \mu_0$, the chosen function implies both the gradual variation in $\mu(\theta)$ and occurrence of short periods of the contact break (when $\mu(\theta) < 0$)). For the choice of the other model parameters, we used the previously obtained experimental data on nonlinear-acoustic properties of granular media [23–25], which indicated that, for the sounding intensity similar to that in the below-described experiments, the weak-contact fraction oscillated in the clapping regime and the characteristic value of the unloading parameter was estimated as $\mu \sim 0.01$. Thus in eq. (1), we assumed $\mu = 0.01$ and the primary acoustic-signal amplitude equal to $2\mu\varepsilon_0$. Figure 2 shows the variations in the fundamental acoustic-stress component $\tilde{\sigma}_\omega$ and the nonlinear-signal components $\tilde{\sigma}_\Omega$ or $\tilde{\sigma}_{2\omega}$ predicted using eq. (1). For the fundamental component, the expected variability is much smaller than that for the nonlinear component which reaches several dB. It is seen in fig. 2 that the shape of the nonlinear-signal variability shows clear correspondence with the variability of the unloading parameter μ for the weak contacts, whereas the increasing depth of the nonlinear-signal variations is proportional to the number of the mobilized contacts which experience rearrangements.

The described idea to detect the weak-contact rearrangements by observing the variability of the nonlinearity-induced component(s) of the sounding signal was implemented in the conditions similar to those used in [8]. Glass beads ((3 ± 0.1) mm) were placed into a $20 \times 30 \times 11$ cm plexiglas box which could be slowly tilted by a motor via a pulley system. The bead-layer thickness was about 8 cm. Through the holes in the opposite longer sides of the box, two identical

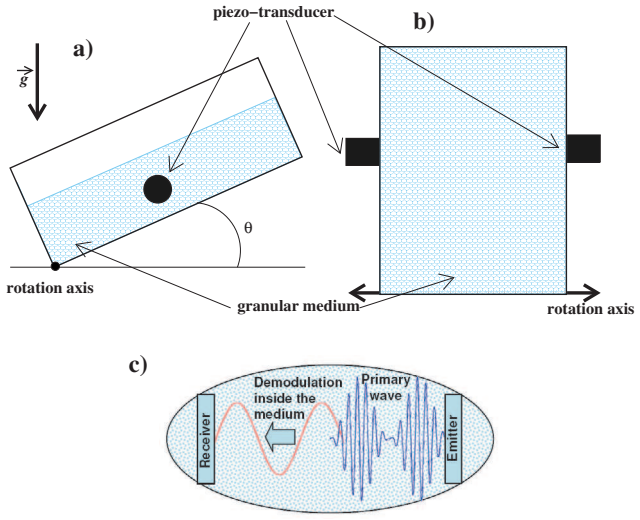

Fig. 3: Sketch of the experimental setup (side-view (a) and top-view (b)). A $20 \times 30 \times 10$ cm plexiglass box filled with glass beads (diameter of 3 ± 0.1 mm) is slowly tilted via a pulley system (not shown). Through holes in the opposite longer sides of the box, two identical emitting-receiving piezo-transducers were fixed. (c) Schematically shown demodulation process in the material bulk.

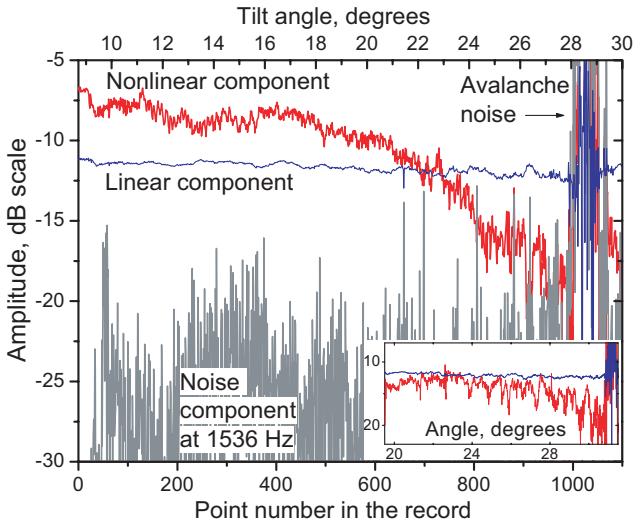

Fig. 4: Examples of the signal temporal slices made in a wider angular range of 8.7°–30° and another more detailed record for last 9° before the avalanche (in the inset).

emitting-receiving piezo-transducers with 40 mm diameter were fixed (see fig. 3). Among different nonlinear effects interesting for diagnostic applications (higher harmonic generation [23,25], cross-modulation [26], burst-signal demodulation [24], etc.) we chose the demodulation of a 100% amplitude-modulated sinusoidal signal. This provided the demodulated energy concentration in a narrow frequency band and ensured much smaller attenuation compared to the case of the second-harmonic generation. The chosen primary carrier frequency 9472 Hz and the modulation one 1024 Hz ensured the reasonable trade-off between the separation from the motor noise (localized below 300–500 Hz) and the radiation efficiency. The received signal was Fourier-transformed thus resolving the fundamental and demodulated components and allowing us to observe additionally bead-rearrangement–produced noise components (of which we recorded 640 Hz and 1536 Hz lines). We made temporal slices of the chosen lines in series of 1110 spectra recorded with a time step of 39.05 ms, which sufficed to observe transitional signal variations due to bead rearrangements. In what follows, in order to give a clear representation on the time scales of the observed structural variations, we intentionally keep on the plots the indication of the data-point numbers together with the indication of the corresponding tilt angles.

Observation results. – A typical example of the obtained temporal slices is given in fig. 4 where for the clarity only one (1536 Hz) noise component is left. The inset presents in more detail several quasi-periodic signal variations closer to the avalanche triggering, which show the remarkable resemblance with fig. 2 and correspond to collective weak-contacts rearrangements with increasing strength. The difference in the pre-avalanche variability of the fundamental and demodulated components also well agree with fig. 2. However, for the noise, only some of the abrupt maxima coincided with rapid variations in the nonlinear signal coming from the material bulk, whereas noise bursts in the beginning of the record in fig. 4 evidently were caused by bead rearrangements on the surface and determined by its profile. This comparison allows for separation of surface and volume effects.

In more detail for last 8°–10° before the avalanche, nonlinear signal variations due to collective contact rearrangements closer to the critical angle are shown in fig. 5(a) (which is similar to the inset in fig. 4). The average visible periodicity of the nonlinear signal variations is about 0.7° for fig. 5(a) and 0.5° for the inset in fig. 4. This can be compared with the angular Fourier spectrum of these variations. In order to reduce the contribution of the zero harmonic (corresponding to the background invariable contribution of the contacts), we subtracted the base-line from the signal amplitude (fig. 5(a)) so that only variations with zero total area were left. The corresponding resultant spectra (fig. 5(b)) demonstrate a pronounced multi-component discrete structure. The most intensive peaks at 0.6° and 0.5° in fig. 5(b) agree well with the main visible periods of the nonlinear "precursors" in figs. 5(a) and 4. There are also peaks consistent with $1.8° \pm 0.4°$ periodicity of the on-surface precursors reported in [8]. Certainly, exacts details of the signal variations did not coincide for different experimental runs, but the main features (first, relatively small-amplitude variations and then several larger-scale clearly seen quasiperiodical precursors with increasing intensity) were well reproducible.

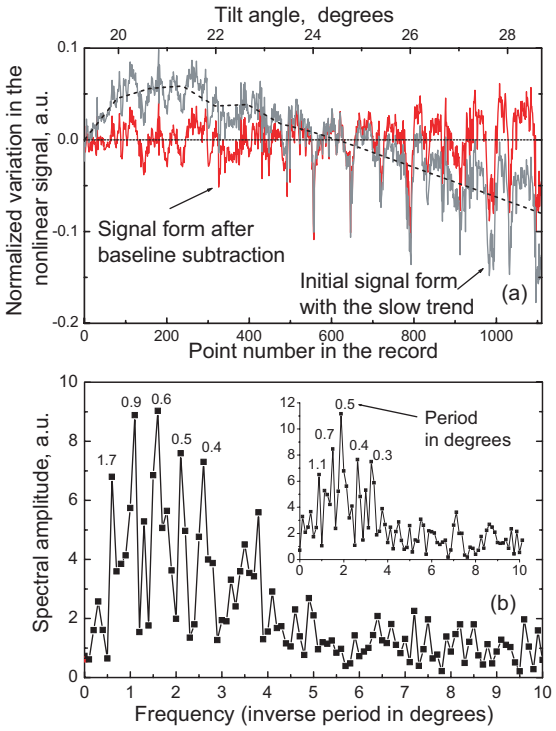

Fig. 5: Nonlinear signal variability for last 9° before the critical angle (a) and its Fourier spectrum (b) exhibiting consistent periodicity. The inset corresponds to the inset in fig. 4.

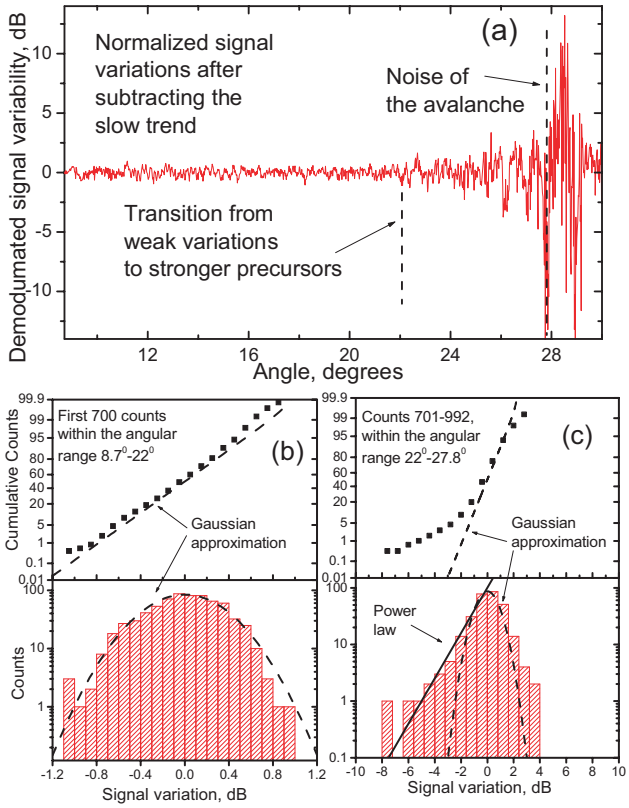

Fig. 6: Normalized variations of the nonlinear signal (a) (the same as shown in fig. 4 in the non-normalized form) and statistical distributions of the variations for the first part (1–700 points) and the second part (701–992 points) of the record before and after appearance of the precursors, respectively.

Consider now statistical properties of the demodulated-signal variations taking as an example the record shown in fig. 4. After subtraction of the slow trend and normalization, the signal variations are shown in fig. 6(a), where two regions with essentially different character are clearly seen. Below tilt angle 22°, the jitter-like variations have no clear periodicity, which clearly appears closer to the critical angle. Bearing in mind further comparison with the data [8], where the event statistics were presented for uniform bin-size in the log-amplitude scale, we also make the same (although for variations < 1 dB, the result is almost the same as in the linear scale, since $\ln(1+x) \approx x$). The so-found statistical properties shown (fig. 6(b) and (c)) demonstrate remarkable difference between the above-mentioned regions. The weak variations have near-Gaussian statistics, whereas the stronger variations in the range 22°–28° shown in fig. 6(c), exhibit rather power law behavior. This transition of the signal coming from pre-avalanche rearrangements in the material bulk from initially Gaussian to power law statistics agrees with observations [8] of the on-surface rearrangements.

Furthermore, the proposed technique revealed active structural rearrangements even in the motionless granular material up to 10–30 minutes after avalanche. Figure 7 shows such records made about 10 and 38 (inset) minutes after the avalanche, which demonstrate both the small-amplitude jitter-like variations and less frequent and deeper variations related to collective

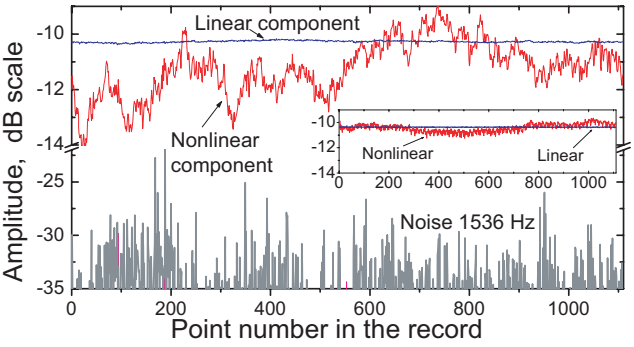

Fig. 7: Pronounced variations in the nonlinear signal recorded 10 min after the avalanche revealing active rearrangements in the apparently motionless packing. The record in the inset (in the same scale) is made 38 min after the avalanche, when the medium has almost reached a new equilibrium (1000 points = 39.05 s).

contact rearrangements. The role of the sounding waves themselves for these variations requires further studies. Nevertheless, since such variations essentially cease as the granular packing approaches a new equilibrium, they indeed give information on the state of the contacts in the packing after an avalanche. Our results based on the

signal coming from the medium bulk generically agree with observations [28] of post-avalanche slowly relaxing bead microdisplacements visible though the transparent wall in the vertical cross-section of the pile.

Conclusions. – This first demonstration of the nonlinear-acoustic monitoring of pre-avalanche instabilities in granular-material bulk confirmed the expected strongly superior sensitivity of the method compared to conventional linear sounding. The proposed technique provides rich information on the state of weak contacts inaccessible to other methods and should stimulate further detailed laboratory studies. For initially intact solid samples, it seems not so surprising that the increased level of nonlinear acoustic effects due to the contact nonlinearity at crack interfaces can be used as a sensitive indicator of the material damage. What looks more striking and even paradoxical is the fact that even in granular materials consisting of inherently strongly nonlinear contacts, the nonlinear acoustic methodology has also proven to be very effective for selective probing of the weakest contacts. Qualitatively, the revealed pre-avalanche quasi-periodicity in the nonlinear signal component and the transition from the nearly Gaussian statistics of the fluctuations to a power law behavior well correlate with the surface data [3,8], simulations [9,10] and agree with general features of complex systems occurring sufficiently far from equilibrium, for example, in processes of granular material compaction [29]. Our (based on the reported here and previous nonlinear-acoustic data [22–26]) representation of granular materials as two-phase systems (comprising strong- and weak-contact networks) well correlate with the similar view based on numerical simulations [30].

The slow relaxation observed after the avalanche is a surprising result that shows the complexity of the notion of stability for a granular packing. Calibrated-amplitude nonlinear sounding opens the possibility to quantify the extent of the weak-contact unloading, whereas comparing the linear and nonlinear signal components allows one to distinguish the modifications of average- and weakly-loaded contact sub-networks. Application of shear waves with different polarizations provides additional possibilities in probing the medium anisotropy (some of these aspects are discussed in more detail in [24–26]). We speculate that besides laboratory applications, the applied method could probably be developed into a useful tool for improving avalanche forecasting in field conditions.

* * *

The study was supported by ANR-project "grANuLar" NT 05-341989 and RFBR grant 06-02-72550CNRS. VYuZ acknowledges the University of Rennes for obtaining the invited-professor grant. We thank A. Valance and S. Kiesgen de Richter for useful discussions and help in the experiment organization and S. McNamara for critical reading of the manuscript.

REFERENCES

[1] Jaeger H. M., Nagel S. R. and Behringer R. P., *Rev. Mod. Phys.*, **68** (1996) 1259.
[2] Aranson I. S. and Tsimring L., *Rev. Mod. Phys.*, **78** (2006) 641.
[3] Bretz M., Cunningham J. B., Kurcynski P. L. and Nori F., *Phys. Rev. Lett.*, **69** (1992) 2431.
[4] Daerr A. and Douady S., *Nature*, **399** (1999) 241.
[5] Dorbolo S., *Eur. Phys. J. E*, **17** (2005) 77.
[6] Scheller T., Huss C., Lumay G., Vandewalle N. and Dorbolo S., *Phys. Rev. E*, **74** (2006) 031311.
[7] Aguirre M. A., Nerone N., Ippolito I., Calvo A. and Bideau D., *Granular Matter*, **3** (2001) 75.
[8] Nerone N., Aguirre M. A., Calvo A., Bideau D. and Ippolito I., *Phys. Rev. E*, **67** (2003) 011302.
[9] Staron L., Vilotte J.-P. and Radjai F., *Phys. Rev. Lett.*, **89** (2002) 204302.
[10] Staron L., Radjai F. and Vilotte J.-P., *J. Stat. Mech.*, **89** (2006) 07014.
[11] Moreau J.-J., *Eur. J. Mech. A-Solids*, **4** (1994) 93.
[12] Blair D. L., Mueggenburg N. W., Marshall A. H., Jaeger H. M. and Nagel S. R., *Phys. Rev. E*, **63** (2001) 041304.
[13] Løvoll G., Måløy K. J. and Flekkøy E. G., *Phys. Rev. E*, **60** (1999) 5872.
[14] Liu C.-h., Nagel S. R., Schecter D. A., Coppersmith S. N., Majmudar S., Narayan O. and Witten T. A., *Science*, **269** (1995) 513.
[15] Majmudar T. S. and Behringer R. P, *Nature*, **435** (2005) 1079.
[16] Kabla A., Debregeas G., Di Meglio G.-M. and Senden T., *Europhys. Lett.*, **71** (2005) 932.
[17] Hardin B. O. and Richart F. E., *J. Soil Mech. Found. Div.*, **89**, No. SM1 (1963) 33.
[18] Domenico S. N., *Geophys.*, **42** (1977) 1339.
[19] Winkler K. W., *Geophys. Res. Lett.*, **10** (1983) 1073.
[20] Gilles B. and Coste C., *Phys. Rev. Lett.*, **90** (2003) 174302.
[21] Makse H. A., Gland N., Johnson D. L. and Schwartz L., *Phys. Rev. E*, **70** (2004) 061302.
[22] Belyaeva I. Yu., Zaitsev V. Yu. and Timanin E. M., *Acoust. Phys.*, **40** (1994) 789.
[23] Zaitsev V. Yu., *Acoust. Phys.*, **41** (1995) 385.
[24] Tournat V., Zaitsev V., Gusev V., Nazarov V., Bequin P. and Castagnede B., *Phys. Rev. Lett.*, **92** (2004) 085502.
[25] Tournat V., Gusev V., Zaitsev V. and Castagnede B., *Europhys. Lett.*, **66** (2004) 798.
[26] Zaitsev V., Nazarov V., Tournat V., Gusev V. and Castagnede B., *Europhys. Lett.*, **70** (2005) 607.
[27] Corwin E. I., Jaeger H. M. and Nagel S. R., *Nature*, **435** (2005) 1075.
[28] Deboeuf S., Bertin E., Lajeunesse E. and Dauchot O., *Eur. Phys. J. B*, **36** (2003) 105.
[29] Ribiere P., Richard P., Delannay R., Bideau D., Toiya M. and Losert W., *Phys. Rev. Lett.*, **95** (2005) 268001.
[30] Deboeuf S., Dauchot O., Staron L., Mangeney A. and Vilotte J.-P., *Phys. Rev. E*, **72** (2005) 051305.